IR and Raman Spectra, Conformational Flexibility, and Scaled Quantum Mechanical Force Fields of Sodium Dimethyl Phosphate and Dimethyl Phosphate Anion†

ARTICLE *in* THE JOURNAL OF PHYSICAL CHEMISTRY · JANUARY 1996

Impact Factor: 2.78 · DOI: 10.1021/jp9520299

Article

IR and Raman Spectra, Conformational Flexibility, and Scaled Quantum Mechanical Force Fields of Sodium Dimethyl Phosphate and Dimethyl Phosphate Anion

Jan Florin, Vladimr Baumruk, Marek trajbl, Lucie Bednrov, and Josef tpnek

J. Phys. Chem., **1996**, 100 (5), 1559-1568 • DOI: 10.1021/jp9520299

IR and Raman Spectra, Conformational Flexibility, and Scaled Quantum Mechanical Force Fields of Sodium Dimethyl Phosphate and Dimethyl Phosphate Anion†

Jan Florián,*,‡,§ Vladimír Baumruk,‡ Marek Štrajbl,‡ Lucie Bednárová,⊥ and Josef Štěpánek‡

Institute of Physics, Charles University, Ke Karlovu 5, CZ-12116 Prague 2, Czech Republic, Department of Chemistry, Jackson State University, Jackson, Mississippi 39217, and Institute of Organic Chemistry and Biochemistry, Academy of Sciences of the Czech Republic, Flemingovo nám. 2, CZ-16610 Prague 6, Czech Republic

Received: July 17, 1995; In Final Form: October 16, 1995⊗

Quantum chemical calculations, involving Hartree−Fock (HF), perturbation (MP2), and density functional (DFT) theories, are carried out for the dimethyl phosphate anion (DMP) and sodium dimethyl phosphate (NaDMP), model systems for the DNA phosphate group. Energies, geometries, and harmonic force fields of different conformations of DMP and NaDMP are compared. In addition, atomic charges derived from the HF/6-31G* and MP2/6-31+G* electrostatic potential of DMP and NaDMP are calculated in order to determine the effects of counterions upon the charge distribution. Finally, IR and Raman spectra of solid and aqueous NaDMP, recorded here in the 80−4000 cm^{-1} (IR) and 150−3100 cm^{-1} (Raman) spectral regions, are assigned using differentially scaled Hartree−Fock, MP2, and B3-LYP force fields of DMP and NaDMP. Our interpretation of the individual vibrational bands confirms the results of the previous empirical normal-coordinate analysis of DMP of Thomas et al. (*Biophys. J.* **1994**, *66*, 225). Also, the predicted frequencies, IR and Raman intensities, depolarization ratios, and ^{13}C isotopic frequency shifts agree well with the experimental data. Among the computational methods, the best results are obtained using the B3-LYP gradient corrected density functional. The proposed scale factors for the HF/3-21G(*), HF/6-31G*, MP2/6-31+G*, and B3-LYP/6-31G* force fields of DMP or NaDMP are transferable to larger systems involving phosphodiester moiety, for example to nucleotides or phospholipids.

Introduction

Sodium dimethyl phosphate (NaDMP) and dimethyl phosphate anion (DMP) represent the smallest realistic model systems of the phosphodiester linkage in nucleic acids and phospholipids. Detailed knowledge of the structure and force fields of these molecules helps to elucidate the relationships between the structure and the function of nucleic acids and phospholipids. Moreover, this information is crucial for biological applications of vibrational spectroscopy and molecular modeling techniques.

Spectral patterns originating from vibrations of the phosphate group are found to be strongly conformationally sensitive. The Raman and IR "marker bands" for A, B, and Z conformations of synthetic oligonucleotides and native DNAs have been recently reviewed by Thomas and Tsuboi,[1] Peticolas,[2] and Taillandier and Liquier.[3] To analyze these spectra, numerous normal-coordinate analyses of dimethyl and diethyl phosphates have been carried out.[4−8] These studies were based on empirical force field parameters fitted to the frequencies from IR and Raman spectra of aqueous solutions and crystalline samples of barium dialkyl phosphates[4,7,9,10] and NaDMP.[8,9] Force constants developed in this way were subsequently transferred by Brown et al.[5,6] and Lu et al.[11] to more extended models of the DNA backbone to study the conformational dependence of frequency shifts. Because the same force constants were used for all conformations studied, such approaches were in principle unable to reveal the most important, dynamic part of the structure−spectra relationships.

The conformation-dependent changes in molecular force fields can be properly described only at the quantum mechanical level. However, the use of rigorous quantum chemical methods is limited only to small molecules. Consequently, for biologically important molecules, several approximations that decrease the accuracy of the calculated vibrational spectra are needed. At the *ab initio* Hartree−Fock (HF) level of theory, these approximations involve the complete neglect of electron correlation effects, and the use of a limited set of basis functions for the construction of molecular orbitals. For mono- and dihydrated DMP and its sodium and ammonium complexes, the HF/3-21G(*) frequencies and spectral assignments have been given by Hadzi et al.[12] The larger 6-31G* basis set was used in HF calculations of IR spectra of DMP in different conformations.[13] Because of these drawbacks, the calculated spectra disagreed with those measured for aqueous solutions or crystalline samples.

Fortunately, the errors associated with electron correlation and basis set effects, and also those caused by the harmonic approximation, exhibit fairly systematic character. For example, the Hartree−Fock (HF) method usually overestimates vibrational frequencies by about 10−15%. Within a given computational method, the errors in diagonal force constants are usually similar for the same types of chemical bonds or bond angles (internal coordinates), although these coordinates belong to different molecules. A regularity of this type, which was noticed by Pulay and Meyer,[14] and by Blom and Altona,[15] has served as basis of the concept of scaled quantum mechanical (SQM) force

* Corresponding author. Current address: Department of Chemistry, University of Southern California, Los Angeles, CA 90089-1062

† This paper is the seventh in the series "Scaled quantum mechanical force fields and vibrational spectra of solid state nucleic acid constituents".

‡ Charles University.

§ Jackson State University.

⊥ Academy of Sciences of the Czech Republic.

⊗ Abstract published in *Advance ACS Abstracts,* December 15, 1995.

0022-3654/96/20100-1559$12.00/0

fields.[16] In this procedure, a set of scale factors, S_i, is used to correct quantum mechanical harmonic force constants F_{ij} according to the equation

$$F'_{ij} = (S_i S_j)^{1/2} F_{ij} \quad (1)$$

The force constants are usually expressed in the standardized internal coordinates[17,18] that enable the transferability of scale factors among related molecules.

Because nucleic acids are composed of repeating subunits of bases, (deoxy)riboses, and phosphates, calculating the vibrational spectra of nucleic acids may be simplified by using the scale factors developed for the individual subunits in the analysis of the whole molecule. Because ab initio force fields can be evaluated for distinct conformations, scaling approaches naturally predict the conformationally dependent spectral variations, and, at the same time, they provide vibrational frequencies accurate enough for finding mutual correlations with experimental bands. For this purpose, the ability of ab initio methods to predict IR and Raman intensities is of great utility.

Work along these lines is in progress in several laboratories. Scale factors of the HF STO-3G, MINI-1, 3-21G, and 6-31G* force fields of nucleic acid bases[19−23] have been determined, and the transferability of these scale factors to protonated and modified nucleic acid bases has been demonstrated. Also, very recently, the scale factors of the HF/3-21+G(*) force field of DMP have been reported.[24] However, in the case of calculations of vibrational spectra and conformational equilibria of DNA phosphodiester moiety, the important role of metal counterions in the stabilization of the DNA duplex by a formation of complexes with negatively charged phosphate group[25] should be taken into account. To date, no ab initio studies of the conformational equilibria of cation−DMP complex have been reported. For the DMP anion, relative stabilities of the gauche−gauche (gg), gauche−trans (gt), and trans−trans (tt) conformations have been evaluated at the HF 3-21G(*), 6-31G*, and 6-31+G* levels.[13,26] These studies, and also Monte-Carlo simulations of aqueous solvation of DMP,[27−31] have shown the gg to be the most stable conformation, followed by gt and tt conformations. The calculated free energy differences indicated that the gt conformer is thermally accessible at ambient temperature. Obviously, this torsional flexibility underlies the DNA polymorphism observed in single crystals[32,33] and solutions.[25]

Of considerable interest is also the performance of newly emerging density functional theory (DFT) methods[34,35] for nucleic acid constituents. These methods include electron correlation effects while being significantly less demanding than conventional approaches such as perturbation or coupled cluster methods. For vibrational spectra of smaller molecules, the DFT calculations appear to be superior to HF methods.[36,37] The errors of DFT force fields have also been shown to be consistent enough to benefit from scaling.[38−40]

The objective of the present paper is threefold. First, we study the electron correlation effects upon the physicochemical properties of the model compounds, dimethyl phosphate anion (DMP) and its complex with Na^+ (NaDMP). For this purpose, we carry out both density functional and Møller−Plesset (MP2) perturbation calculations of the vibrational spectra, energies, and geometries of gauche−gauche, gauche−trans, and trans−trans conformers of these systems. In addition, energy barriers (transition states) between these minima on the potential energy surface are evaluated. Second, in order to enable vibrational analyses of larger systems involving phosphate groups, via the transferability of scale factor, we adjust scale factors of the HF/3-21G(*), HF/6-31G*, MP2/6-31+G*, and Becke3-LYP/6-31G* force fields using the frequencies observed for NaDMP in the solid state and aqueous solutions. Finally, we check the reliability of the calculated spectra by comparison to the IR and Raman spectra of solid and liquid NaDMP measured by us, and with the spectra of ^{13}C isotopically substituted NaDMP.[8] The IR spectrum of aqueous solution of NaDMP is presented for the first time in this study. The other spectra have been published before,[8,9] but for smaller frequency regions.

Experimental Methods

Dr. Ivan Rosenberg from the Institute of Organic Chemistry and Biochemistry, Academy of Sciences of the Czech Republic, kindly provided us with a sample of sodium dimethyl phosphate.

Raman Spectroscopy. Raman spectra of polycrystalline sodium dimethyl phosphate in the 150−3100 cm^{-1} spectral region were collected on a single channel spectrometer at 1 cm^{-1} intervals with an integration time of 6 s, using a spectral slit width of 3 cm^{-1}. Spectra of 1.0 M solution were measured on a multichannel Raman spectrometer with a CCD detection system having 1024 pixels along dispersion axis. Raman spectra were excited with the 488 nm line of argon laser using approximately 200 mW of radiant power at the sample, and collected in the 350−1750 and 2200−3500 cm^{-1} intervals with a 6 cm^{-1} spectral slit width and an accumulation time of 200 s. The spectral frequencies were calibrated with argon ion laser plasma lines and are believed to be accurate to ±1 cm^{-1}. For collection of the parallel and perpendicular components of the polarized Raman spectra of solution samples, a plane of polarization of the incident beam was rotated and the orientation of a polarizing analyzer located between the sample and the entrance slit of the spectrograph was kept fixed. Solvent spectrum in the O−H stretching region was carefully subtracted. Peak positions were determined by a curve-fit procedure using a SpectraCalc software.

Infrared Spectroscopy. Infrared spectra of sodium dimethyl phosphate in KBr pellets were recorded with a Nicolet Impact 400 FTIR spectrometer. The spectra in the region from 400 to 4000 cm^{-1} were collected with a standard source, a KBr beam splitter, and a DTGS detector. Spectra of 1.0 M solution of sodium dimethyl phosphate in H_2O were measured in a demountable cell (Graseby Specac) consisting of a pair of CaF_2 windows separated by a 6 μm Mylar spacer. Solvent spectrum was carefully subtracted. Generally, 512 scans were collected with a spectral resolution of 2 cm^{-1} and Happ-Genzel apodization function.

Spectra in the far IR region from 80 to 550 cm^{-1} were measured in CsI pellets on a Bruker IFS-88 spectrometer with a standard source, a 6 μm Mylar beam splitter, and a DTGS detector. Generally, 512 scans were collected with a spectral resolution of 2 cm^{-1} and Blackmann-Harris three-term apodization function.

No baseline corrections were made. Absorption peak positions were determined by a curvefit procedure using a SpectraCalc software.

Computational Methods

The geometry and harmonic force fields of the gg conformation of DMP were calculated by Hartree−Fock (HF) method, second-order Møller−Plesset perturbation theory (MP2), and density functional theory (DFT). Standard Gaussian basis sets involving the minimal STO-3G and polarized split-valence (3-21G(*), 6-31G*) basis sets were used for HF and DFT calculations. The d-type polarization functions are placed on phosphorus in the 3-21G(*) basis set, and on C, O, and P atoms in the 6-31G* basis set. The 6-31+G* basis set, which involves

additional diffuse basis functions on C, O, and P atoms was used for MP2 and DFT calculations. Quantum chemical calculations were carried out using the Gaussian 92 program.[41]

Two types of nonlocal exchange-correlation functionals were used for the DFT calculations. The first method involved the combination of Becke's exchange functional[42] and Lee−Young−Parr correlation functional[43] (B-LYP). The second DFT method, denoted B3-LYP, employed Becke's three-parameter hybrid functional[44] that consists of HF + nonlocal exchange and correlation parts.

The conformational space of NaDMP was investigated using the HF/6-31G* and B3-LYP/6-31G* full gradient optimization methods. MP2/6-311G* single-point energy calculations were carried out at geometries of stationary points determined at the B3-LYP level. The character of the calculated stationary points was checked by subsequent calculations of the matrix of energy second derivatives (harmonic force constants).

The effective atomic charges were determined by fitting to the electrostatic potential calculated from the HF/6-31G* and MP2/6-31+G* density on a grid, which consisted of 768 and 828 points for DMP and NaDMP, respectively. The grid points were chosen according to the method of Singh and Kollman[45,46] implemented in the Gaussian 92 program.

IR and nonresonant Raman spectra of DMP and NaDMP were computed using the assumption of mechanical and electrical harmonicity of atomic displacements from their equilibrium positions. Within this approximation, IR and Raman intensities are quadratic functions of the normal-coordinate derivatives of the molecular electric dipole moment and polarizability, respectively. The normal modes and frequencies were determined by diagonalization of matrix of the empirically scaled force constants. The unscaled force constants and derivatives of the components of the dipole moment and the polarizability tensor were evaluated in Cartesian coordinates by the quantum chemical methods described above. Because the calculation of the polarizability derivatives by DFT and MP2 methods is not feasible within the Gaussian 92 program, we calculated Raman intensities by combining SQM force fields with the Cartesian dipole and polarizability derivatives obtained at the HF level with the 6-31G+G** and 6-31++G** basis sets.

For calculations of vibrational spectra, the Cartesian force constant matrix was transformed into standard internal coordinates, which observe local symmetry.[18] The diagonal force constants expressed in internal coordinates were scaled by the scale factors adjusted in such a way that calculated and experimental vibrational frequencies matched as closely as possible. This manual approach that avoided the standard least-squares fit determination of scale factors was made possible by the high quality of the unscaled MP2 force field resulting in a low number of independent scale factors. In addition, this technique may also incorporate other spectral characteristics, such as depolarization ratios, ^{13}C frequency shifts, and intensities. Off-diagonal elements of the force constant matrix were multiplied (scaled) by scale factors equal to the geometric mean of the corresponding diagonal scale factors. The program MOLVIB[47] and our program SQMVIB[48] were used.

The latter program was also employed for calculation of IR and Raman intensities. The standard expression based on the double harmonic approximation was used for prediction of IR intensities.[22,49] Raman intensities were calculated for the right angle scattering geometry with the exciting light polarized perpendicularly to the scattering plane and without an analyzer. Raman scattering activity S_j of the j-th normal mode was calculated as

$$S_j = 45\alpha_j^2 + 7\beta_j^2 \quad (2)$$

where α and β are the isotropic and anisotropic invariants of the tensor of polarizability derivatives with respect to j-th normal coordinate.[50,51] Obviously, S_j is independent of experimental conditions such as laser excitation wavenumber (ν_0) or temperature. The inclusion of these effects in the absolute differential Raman scattering cross section[51]

$$\frac{d\sigma_j}{d\Omega} = \frac{2h\pi^2(\nu_0 - \nu_j)^4}{45c\nu_j\left(1 - \exp\left[-\frac{hc\nu_j}{kT}\right]\right)}S_j \quad (3)$$

enhances lower frequencies bands. ν_0, h, c, and k are exciting frequency and universal constants, respectively. In this paper, Raman differential cross sections were calculated for the temperature of 300 K and excitation wavelengths of 488 and 514.5 nm. The calculated spectra were plotted as a sum of Gaussian curves with the half-width of 10 cm^{-1}. Half-width of 20 cm^{-1} was used for simulation of Raman bands assigned to the CH bending vibrations.

Results and Discussion

Conformational Flexibility. Relative stability of different minima on the potential energy surface (PES) represents an important criterion for the evaluation of structural consequences of interactions of counterions with phosphate DNA groups. For description of the different phosphate conformations we adopt notation commonly used in spectroscopy (Figure 1). This convention denotes conformations with COPO (α, ζ) torsional angles of ∼60° as gauche $^+$(g$^+$), those about −60° as gauche $^-$(g$^-$), and those of ∼180° as trans (t). In various nucleotide crystal structures, the torsional angles around P−O bonds exhibit a high degree of flexibility. More specifically, the tg$^-$, g$^-$g$^-$, and g$^+$g$^+$ conformations have been observed for dinucleoside phosphates.[52] In B-DNA Dickerson−Drew self-complementary dodecanucleotide, g$^-$g$^-$ phosphate conformations (B_I) prevail, but alternative g$^-$t phosphate conformation (B_{II}) was observed as well.[53] Finally, the phosphate groups in left-handed Z-DNA double helix exhibit tg$^+$, g$^+$g$^+$, and g$^+$g$^-$ conformations.[54] In DMP and NaDMP, g$^+$g$^+$ and g$^-$g$^-$ conformations are symmetrically equivalent so that they will be denoted as gg. Similarly, gt conformation involves the g$^-$t, g$^+$t, tg$^-$ and tg$^+$ symmetrically equivalent minima.

The *relative energies* of the gg, gt, and tt minima on the potential energy surface (PES) as well as energies of transition states for the gg ↔ gt (TS1), gt ↔ tt (TS2), and gt ↔ tg (TS3) transitions in DMP and NaDMP are compared in Table 1. For the sake of clarity, the calculated α and ζ torsional angles are also presented in this table. In both systems, the gg form was found to be the most stable conformation. Inclusion of electron correlation within either the MP2 or B3-LYP method slightly increases the energy barrier between gg and gt conformers so that it amounts to about 2 kcal/mol. The interaction of DMP with Na^+ slightly stabilizes the gt conformer, but it does not affect the barrier height for the gg ↔ gt transition. The transition between symmetrically equivalent g$^+$t and tg$^-$ structures may proceed either via g$^+$g$^-$ transition state (TS3) of C_s symmetry, or via two TS2 transition states and the tt minimum. Anyway, this conformational transition is less favorable, because it is connected with a ∼2 kcal/mol energy barrier.

The *geometry of the gg conformation* (C_2 symmetry) of the dimethyl phosphate anion and sodium dimethyl phosphate calculated by several quantum chemical methods is given in Table 2. (See Figure 2 for the atom numbering used in this

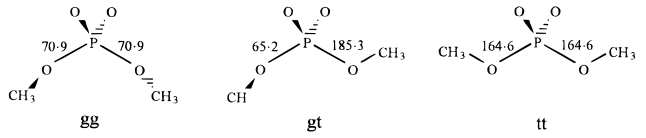

Figure 1. Gauche−gauche (gg), gauche−trans (gt), and trans−trans (tt) conformations of dimethyl phosphate, and the HF/6-31G* P−O torsional angles predicted for sodium dimethyl phosphate.

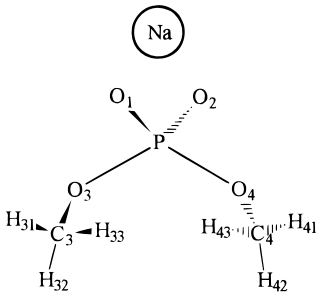

Figure 2. Numbering schemes for DMP and NaDMP. In the text, the "anionic" O1 and O2 atoms are also denoted as O*, and O3 and O4 atoms as O.

study). There are no X-ray results available for sodium dimethyl phosphate. Dimethyl phosphate anion was studied by X-ray diffraction in the complex with $NH4^+$.[55a] As it was shown recently by Guan et al.,[24] ab initio treatment of the ion-pair complex is needed for obtaining satisfactory agreement with experimental structure. Thus, for the purpose of comparison we included crystal structure of barium diethyl phosphate[55b] in Table 2. Obviously, MP2 and DFT methods provide similar geometries. Hartree−Fock calculations utilizing basis sets augmented with polarization functions on phosphorus tend to systematically underestimate P−O* and P−O bond lengths compared to MP2 and DFT ones. On the other hand, the use of the minimal STO-3G basis set results in P−O* and P−O bonds that are systematically too long.

As for the geometry differences between dimethyl phosphate with and without coordinated sodium cation, various computational methods provide similar trends; namely, the P−O* bonds are lengthened and the P−O bonds are shortened in the complex. Also the O*PO* angle narrows from about 125° to 114°, whereas the OPO angle slightly widens. No marked counterion-induced changes were predicted for C−O bonds, including the C−O−P−O torsional angles. With the exception of the O*PO* angle, the B3-LYP geometry of NaDMP agrees well with the crystal structure of barium diethyl phosphate.[55] The discrepancy in the O*PO* angle is most probably due to the smaller ionic radius of the sodium ion.

The *geometries of the gt and tt conformers* of DMP and NaDMP calculated at the HF and B3-LYP levels using the 6-31G* basis set are presented in Table 3. They are comparable with the geometries of the gg conformations given in Table 2. Both theoretical methods provide qualitatively the same geometry variations among different conformations. For example, the P−O bonds gauche to the C−O bonds are found to be slightly longer than those that are trans to C−O bonds. The same trend was previously observed and thoroughly discussed for DMP by Liang et al.[13] The sodium ion is only slightly displaced from the O*PO* plane in the gt conformation. Moreover, it lies on the C_2 symmetry axis for gg and tt conformations. These results agree with the experimental findings of Stangret and Savoie[56] who studied by vibrational spectroscopy interactions of various metal cations with diethyl phosphate in aqueous solution. Their study revealed that interactions of alkaline metal ions with charged phosphate group are of electrostatic nature and that they are essentially symmetrical with respect to the two anionic oxygen atoms.

Due to the minimal differences in the conformational flexibility of DMP and NaDMP, the complexation of positive counterions with the phosphate DNA group will have only minimal effect on the backbone conformation, provided long-range electrostatic interactions between neighboring phosphate groups and also phosphate-ribose interactions can be neglected. The evaluation of such effects is beyond the scope of this paper. Nonetheless, we present in Table 4 several sets of *effective atom charges* for both DMP and NaDMP. These changes might be helpful in future DNA simulations based on empirical force fields. The charges calculated here for DMP are close to those from the second generation AMBER force field.[57] Interestingly, the presence of the counterion does not influence charges on anionic oxygens (O*) but decreases the positive charge on phosphorus at the expense of ester oxygens (O), which become less negative. These changes bring the atomic charges to a closer agreement with the charges derived from electron density of deoxycytidine-5′-monophosphate monohydrate zwitterion determined using high-resolution X-ray diffraction.[58]

Force Constants and Scale Factors. Table 5 shows the unscaled *force constants (FCs)* of the gg conformer of DMP expressed in internal coordinates (Table 6). The first two columns of Table 5 pertain to the HF calculations in 3-21G(*) and 6-31G* basis sets; the remaining columns include MP2 and DFT results obtained with the larger 6-31+G* basis set. Though there are notable differences among FCs calculated by different computational methods the relative magnitudes of FCs related to different internal coordinates are method independent.

The MP2 and B3-LYP force fields are nearly identical. This is an encouraging finding, indicating that basis set truncation errors are small for 6-31+G* basis set. The use of the B-LYP functional results in slightly lower values of stretching FCs

TABLE 1: Relative Stabilities and P−O Torsional Angles of the Structures Corresponding to the Minima and Transition States (TS) on the Potential Energy Surface of DMP and NaDMP

	relative energy (kcal/mol) (α, ζ) (deg)[a]					
method	gg	TS1	gt	TS2	tt	TS3 (g^+g^-)
			DMP			
HF/6-31G*	0.0 (75.1)	1.71 (74.2, 136.4)[c]	1.15 (73.8, 189.4)	2.79 (145.9, 160.2)	2.78 (156.9)	2.67 (94.8)
MP2/6-31+G*[b]	0.0	2.26	1.45		3.66	
			NaDMP			
HF/6-31G*	0.0 (70.9)	1.73 (66.5, 129.3)	0.91 (65.2, 185.3)	3.03 (135.0, 163.0)	2.92 (164.6)	3.05 (86.3)
B3-LYP/6-31G*	0.0 (69.3)	1.83 (65.5, 129.6)	1.09 (65.7, 193.5)	2.68 (132.2, 156.5)	2.58 (154.0)	2.77 (86.5)
MP2/6-311G*[d]	0.0	1.97	1.07	3.65	3.64	3.04

[a] α and ζ correspond to the $O_4PO_3C_3$ and $O_3PO_4C_4$ torsional angles, respectively. ζ = α for gg and tt conformers (C_2 symmetry), and ζ = −α for TS3 (g^+g^- conformer), which possess C_s symmetry. [b] Single-point energy calculations in HF/6-31+G* geometry (ref 13). [c] Reference 13. Note that an incorrect angle α (78.8°) has been given in ref 13 for HF/6-31G* geometry of gt conformer of DMP. [d] Single-point energy calculations in B3-LYP/6-31G* geometry.

TABLE 2: Comparison of Calculated Geometries of Dimethyl Phosphate Anion (DMP) and Sodium Dimethyl Phosphate (NaDMP) with X-ray Geometry of Barium Diethyl Phosphate (BaDEP)

	DMP							NaDMP				BaDEP
parameter[a]	sto3g[b]	321g*	631g*	mp2	blyp	b3lyp	b31yp$^+$	sto3g	321g*	631g*	b31yp	experiment[c]
P−O*	1.582	1.473	1.470	1.509	1.522	1.498	1.504	1.612	1.498	1.491	1.521	1.52, 1.52
P−O	1.731	1.634	1.642	1.684	1.714	1.683	1.682	1.685	1.589	1.597	1.632	1.59, 1.62
O−C	1.422	1.435	1.393	1.427	1.437	1.412	1.418	1.431	1.455	1.412	1.433	1.44, 1.47
C3−C4	4.208	3.918	3.907	3.787	3.953	3.837	3.905	3.888	4.051	3.886	3.872	
O*−Na								1.984	2.161	2.222	2.221	
O*PO*	128.8	124.6	124.9	125.9	125.8	125.7	125.5	106.2	111.9	113.5	114.1	121.6
OPO	95.8	98.3	99.3	98.9	99.6	98.7	99.5	100.5	103.4	103.4	103.5	103.5
POC	112.3	118.2	118.5	115.6	117.0	116.4	117.5	112.7	121.3	120.3	118.0	116, 118
OPOC	87.3	74.8	75.1	69.8	72.2	71.8	72.6	73.3	74.4	70.9	69.3	68.2, 71.6

[a] Bond lengths in angstroms, angles in degrees. The calculated structures of DMP and NaDMP posess C_2 symmetry. Na^+ is positioned at the symmetry axis. [b] The computational methods are denoted as follows: sto3g = HF/STO-3G, 321g* = HF/3-21G(*), 631g* = HF/6-31G*, mp2 = MP2/6-31+G*, blyp = B-LYP/6-31+G*, b31yp = B3-LYP/6-31G*, b3lyp$^+$ = B3-LYP/6-31+G*. [c] Crystal structure of barium diethyl phosphate (ref 55b). The crystal structure of BaDEP is slightly distorted from C_2 symmetry.

TABLE 3: Geometry of the gt and tt Conformers of NaDMP

	HF/6-31G*		B3-LYP/6-31G*	
parameter	gt	tt	gt	tt
bond length (Å)				
P−O	1.499	1.499	1.531	1.530
P−O_2	1.491	1.499	1.521	1.530
P−O_3	1.585	1.588	1.619	1.623
P−O_4	1.598	1.588	1.633	1.623
O_1−Na	2.218	2.206	2.216	2.204
O_2−Na	2.209	2.206	2.215	2.204
O_3−C_3	1.412	1.407	1.432	1.427
O_4−C_4	1.407	1.407	1.427	1.427
angle (deg)				
O_1PO_2	111.9	110.5	112.7	111.3
O_3PO_4	100.2	97.4	99.5	96.4
PO_1Na	89.6	90.7	88.5	89.3
PO_2Na	90.2	90.7	88.7	89.3
PO_3C_3	121.2	120.5	118.8	118.7
PO_4C_4	120.3	120.5	118.3	118.7
torsional angle (deg)				
O_1NaPO_2	174.8	180.0	175.8	180.0
$O_3PO_4C_4$	185.3	164.6	193.5	154.0
$O_4PO_3C_3$	65.2	164.6	65.7	154.0
$O_1PO_2O_3$	−124.7	−125.3	−125.1	−125.7
$O_1PO_2O_4$	124.8	126.3	125.6	127.2

TABLE 4: Electrostatic Potential Derived Atomic Charges (au) of DMP and NaDMP

	DMP(gg)		NaDMP(gg)	
atom	HF[a]	MP2	HF	MP2
P	1.28	1.26	1.04	0.94
O*	−0.81	−0.80	−0.83	−0.79
O	−0.52	−0.51	−0.37	−0.35
C	0.19	0.24	−0.01	0.02
H	0.00	−0.02	0.08	0.065
Na			0.91	0.91

[a] HF and MP2 denote HF/6-31G*//HF/6-31G* and MP2/6-31+G*//HF/6-31G* methods (MEP//geometry), respectively.

whereas B-LYP torsional FCs are significantly larger than their corresponding MP2 and B3-LYP values.

As expected, HF methods provide overestimated diagonal force constants. This trend is consistently retained also for most interaction (off-diagonal) FCs, so that these FCs can be improved by scaling procedure. More detailed analysis of this type has recently been reported for formamide.[38] As with DMP, the formamide force field, calculated at HF level of theory using polarized basis sets, was shown to benefit from Fogarasi−Pulay type of scaling.

The diagonal FCs of gg, gt, and tt conformers of NaDMP, calculated using HF/6-31G* method, are compared in Table 7. Except for PO torsion, variations in magnitudes of FCs among different conformers fall below 4%. These changes are capable of inducing 2% frequency shifts, but they were completely neglected in previous attempts to predict conformational dependence of vibrational spectra of model systems for DNA phosphate linkages and phospholipids, which were based on the empirical normal-coordinate analyses.[5−7,11]

By comparing HF/6-31G* FCs of DMP and NaDMP, presented in Tables 5 and 7, one can get information about FC variations induced by interactions with the sodium ion. Obviously, the most pronounced changes concern the PO*, CO, and PO stretching (ν) FCs; the former two decrease, and the ν(PO) FC increases as a result of the complex formation. Among the bending vibrations of the phosphate group, the δ(PO12) one is significantly larger, and the remaining ones are slightly smaller in NaDMP compared to DMP.

As expected, *scale factors* of the force fields of DMP (Table 8), developed using the experimental spectra of NaDMP, induce similar changes in the stretching FCs as the presence of the sodium ion. Thus, scale factors for DMP tend to effectively include a part of the complexation effects. On the other hand, FCs directly associated with the vibrations of Na atom, as well as the δ(PO12) force constant, seem to be overestimated in the NaDMP model. Consequently, these FCs were decreased by scaling procedure (Table 8). Because of the important role of scaling in either mimicking or dumping the counterion effects, scale factors presented in Table 8 are not directly transferable between DMP and NaDMP. However, a good transferability of these scale factors to larger molecular systems as ribosophosphates can be expected.

Recently, Rauhut and Pulay developed a universal set of scale factors for B3-LYP/6-31G* force fields of organic molecules involving C, N, O, and H atoms.[40] Because their set of "training molecules" included heterocyclic molecules, amino and carbonyl groups, as well as furan, these scale factors, when complemented by scale factors for PO bonds derived by us, might be applicable for the predictions of vibrational spectra of oligonucleotides.

Vibrational Spectra. Table 9 shows harmonic frequencies, ^{13}C frequency shifts, IR and Raman intensities, Raman depolarization ratios, and spectral interpretations, which were calculated by two independent computational methods. These results are compared with the experimental data measured from aqueous solution and solid NaDMP in Table 9 and Figures 3 and 4. The calculated data originate from the scaled quantum mechanical (SQM) MP2 and B3-LYP force fields of DMP and NaDMP, respectively. The purpose of this comparison is to examine whether the force fields of phosphate anions, when properly scaled, are capable of predicting the vibrational spectra of phosphate linkages in native DNA and RNA. Since

TABLE 5: Comparison of the Harmonic Force Constants of the gg Conformer of DMP

FC type[a]	321g*[b]	631g*	mp2	blyp$^+$	b31yp$^+$
diagonal FCs					
ν(PO1)	11.513	10.930	8.746	7.579	8.574
ν(PO3)	5.710	4.953	3.830	2.988	3.679
ν(O3C)	6.031	6.819	5.557	4.877	5.473
δ(POr)	1.774	1.703	1.383	1.473	1.370
δ(POt)	1.357	1.228	1.016	1.112	1.002
δ(POw)	2.388	2.302	1.827	1.892	1.801
δ(PO12)	1.890	1.835	1.446	1.473	1.412
δ(PO34)	1.841	1.776	1.509	1.523	1.426
δ(O3C)	1.109	1.079	1.045	1.114	0.945
σ(PO3)	0.065	0.092	0.119	0.259	0.092
ν(C3Hs)	5.928	5.925	5.473	5.022	5.252
ν(C3Ha1)	5.779	5.761	5.378	4.860	5.092
ν(C3Ha2)	5.609	5.626	5.328	4.799	5.023
δ(C3Hr1)	0.976	1.029	0.896	0.901	0.876
δ(C3Hr2)	0.984	1.060	0.923	0.925	0.901
δ(C3Hs)	0.799	0.801	0.719	0.704	0.690
δ(C3Ha1)	0.732	0.718	0.627	0.625	0.609
δ(C3Ha2)	0.742	0.722	0.635	0.632	0.615
τ(C3H)	0.030	0.034	0.034	0.151	0.039
stretch−stretch interaction FCs					
ν(PO1)−ν(PO2)	0.164	0.242	0.167	0.143	0.168
ν(PO1)−ν(PO3)	0.362	0.368	0.230	0.206	0.237
ν(PO1)−ν(PO4)	0.277	0.329	0.220	0.194	0.226
ν(PO1)−ν(O3C)	−0.105	−0.137	−0.103	−0.092	−0.101
ν(PO1)−ν(O4C)	−0.045	−0.056	−0.040	−0.044	−0.048
ν(PO3)−ν(PO4)	0.437	0.435	0.302	0.250	0.288
ν(PO3)−ν(O3C)	0.200	0.250	0.175	0.200	0.221
ν(PO3)−ν(O4C)	−0.084	−0.094	−0.074	−0.073	−0.073
stretch−bend interaction FCs					
ν(PO1)−δ(O3C)	0.025	−0.021	−0.032	−0.020	−0.029
ν(PO1)−δ(O4C)	0.037	0.057	0.057	0.048	0.056
ν(PO1)−δ(PO12)	0.104	0.138	0.091	0.080	0.088
ν(PO1)−δ(PO34)	−0.148	−0.151	−0.105	−0.109	−0.118
ν(PO1)−δ(POr)	0.363	0.376	0.293	0.266	0.286
ν(PO3)−δ(O3C)	0.515	0.434	0.422	0.370	0.391
ν(PO3)−δ(PO12)	−0.257	−0.253	−0.209	−0.166	−0.191
ν(PO3)−δ(PO34)	0.323	0.319	0.271	0.209	0.235
ν(PO3)−δ(POw)	−0.545	−0.524	−0.405	−0.363	−0.397
ν(O3C)−δ(O3C)	0.694	0.567	0.560	0.455	0.512
ν(O3C)−δ(PO34)	−0.108	−0.090	−0.098	−0.099	−0.088
ν(O3C)−δ(POr)	−0.123	−0.061	−0.094	−0.093	−0.088
ν(O3C)−δ(POt)	0.084	0.061	0.090	0.095	0.076
ν(O3C)−δ(POw)	0.072	0.092	0.054	0.048	0.056
bend−bend interaction FCs					
δ(PO12)−δ(O3C)	−0.076	−0.053	−0.039	−0.035	−0.037
δ(PO12)−δ(PO34)	−0.063	−0.102	−0.060	−0.057	−0.055
δ(PO12)−δ(POt)	0.080	0.063	0.039	0.032	0.042
δ(PO34)−δ(POt)	−0.039	−0.008	−0.031	−0.069	−0.019
δ(POr)−δ(O3C)	−0.021	−0.029	−0.039	0.035	−0.045
δ(POw)−δ(O3C)	−0.086	−0.075	−0.076	−0.064	−0.071
δ(POw)−δ(POr)	−0.116	−0.082	−0.042	−0.032	−0.044

[a] Stretching, bending, and stretch−bend force constants in mdyn/Å, mdyn, and mdyn·Å, respectively. Only symmetrically unique interaction FCs whose MP2 absolute values are larger than 0.03 mdyn/Å (mdyn, mdyn·Å) and which do not involve internal coordinates of CH_3 groups are presented. Definition of internal coordinates is given in Table 6. [b] For abreviation of computational methods see Table 2.

interactions with counterions play an important role in native nucleic acids, the vibrational spectra of NaDMP are predicted as well. Though the NaDMP-based force fields could be intuitively expected to provide better results, the neglect of solvation effects could result in overestimation of the impact of Na^+ on vibrational spectra. Moreover, the use of models based on DMP is attractive due to their smaller size.

Vibrational bands observed in the *80−600 cm^{-1} frequency region* belong to the bending and torsional vibrations of methyl and phosphate groups. Because no experimental spectra of NaDMP have been reported below 150 cm^{-1}, bands predicted to lie in this region can be verified only by comparison with

TABLE 6: Definition of Internal Coordinates of Dimethyl Phosphate and Sodium Dimethyl Phosphate

coordinate[a]	description	definition[b]
ν(PO1)	PO* stretching	$\Delta r_{P,O1}$
ν(PO3)	PO stretching	$\Delta r_{P,O3}$
ν(PNa)	PNa stretching	$\Delta r_{P,Na}$
ν(O3C)	OC stretching	$\Delta r_{O3,C3}$
δ(PO12)	O*PO* bending	$\Delta\alpha_{O1,P,O2}$
δ(PO34)	OPO bending	$\Delta\alpha_{O3,P,O4}$
δ(POw)	O*PO* wagging	$\Delta\alpha_{O1,P,O4} + \Delta\alpha_{O2,P,O4} - \Delta r_{O1,P,O3} - \Delta r_{O2,P,O3}$
δ(POr)	O*PO* rocking	$\Delta\alpha_{O1,P,O4} - \Delta\alpha_{O2,P,O4} + \Delta\alpha_{O1,P,O3} - \Delta\alpha_{O2,P,O3}$
δ(POt)	O*PO* twisting	$\Delta\alpha_{O1,P,O4} - \Delta\alpha_{O2,P,O4} - \Delta\alpha_{O1,P,O3} + \Delta\alpha_{O2,P,O3}$
δ(PNa1)	O*PNa bending	$\Delta\alpha_{Na,P,O1} - \Delta\alpha_{Na,P,O2}$
δ(PNa2)	OPNa bending	$\Delta\alpha_{Na,P,O3} - \Delta\alpha_{Na,P,O4}$
δ(O3C)	POC bending	$\Delta\alpha_{C3,O3,P}$
ν(C3Hs)	CH_3 sym stretching	$\Delta r_{C3,H31} + \Delta r_{C3,H32} + \Delta r_{C3,H33}$
ν(C3Ha1)	CH_3 asym stretching	$2\Delta r_{C3,H31} - (\Delta r_{C3,H32} + \Delta r_{C3,H33})$
ν(C3Ha2)		$\Delta r_{C3,H31} - \Delta r_{C3,H33}$
δ(C3Hr1)	OCH_3 rocking	$2\Delta\alpha_{O3,C3,H31} - (\Delta\alpha_{O3,C3,H32} + \Delta\alpha_{O3,C3,H33})$
δ(C3Hr2)		$\Delta\alpha_{O3,C3,H32} - \Delta\alpha_{O3,C3,H33}$
δ(C3Hs)	CH_3 sym bending	$\Delta\alpha_{H31,C3,H32} + \Delta\alpha_{H32,C3,H33} + \Delta\alpha_{H33,C3,H31} - \Delta\alpha_{O3,C3,H31} - \Delta\alpha_{O3,C3,H32} - \Delta\alpha_{O3,C3,H33}$
δC3Ha1	CH33 asym bending	$2\Delta\alpha_{H32,C3,H33} - (\Delta\alpha_{H31,C3,H32} + \Delta\alpha_{H33,C3,H31})$
δC3Ha2		$\Delta\alpha_{H31,C3,H32} - \Delta\alpha_{H33,C3,H31}$
τPO3	PO torsion	$1/3(\Delta\tau_{C3,O3,P,O4} + \Delta\tau_{C3,O3,P,O1} + \Delta\tau_{C3,O3,P,O2})$
τC3H	CH_3 torsion	$1/3(\Delta\tau_{H31,C3,O3,P} + \Delta\tau_{H32,C3,O3,P} + \Delta\tau_{H33,C3,O3,P})$

[a] Coordinates observing local symmetry. Only coordinates for the structurally unique part of the molecule are given. The definition of internal coordinates for the other part of the molecule was done analogously. [b] The symbols r, α, and τ denote bond length, bond angle, and torsional angle, respectively. The value of the atom 1−atom 2−atom 3−atom 4 torsional angle is defined as the angle between projections of the atom 1−atom 2 and atom 3−atom 4 bonds on the plane perpendicular to the central, atom 2−atom 3, bond. It is possitive when the more distant bond, viewed in the direction of the central bond, is rotated clockwise from the eclipsed (cis) arrangement. For atom numbering see Figure 2.

TABLE 7: Conformational Dependence of the Diagonal HF/6-31G* Force Constants[a] of Sodium Dimethyl Phosphate

FC	gg	gt	tt
ν(PO1)	9.833	9.468	9.451
ν(PO2)	9.833	9.819	9.451
ν(PO3)	6.090	6.446	6.366
ν(PO4)	6.090	6.065	6.366
ν(PNa)	1.207	1.225	1.245
ν(O3C)	6.297	6.309	6.442
ν(O4C)	6.297	6.434	6.442
δ(PO12)	2.631	2.753	2.872
δ(PO34)	1.753	1.857	1.909
δ(POw)	2.306	2.353	2.429
δ(POr)	1.646	1.581	1.537
δ(POt)	1.094	1.012	0.969
δ(PNa1)	1.042	1.121	1.197
δ(PNa2)	0.194	0.224	0.262
δ(O3C)	0.883	0.867	0.842
δ(O4C)	0.883	0.825	0.842
τ(PO3)	0.087	0.074	0.020
τ(PO4)	0.087	0.035	0.020

[a] Unscaled values, in mdyn/Å and mdyn·Å for stretching and bending (torsional) FC types, respectively.

the spectra of barium dimethyl phosphate[7] (Table 9). Both the MP2 (DMP) and B3-LYP (NaDMP) calculations agree in that the lowest-frequency phosphate modes near 100 cm^{-1} correspond to the in-phase and out-of-phase combinations of

TABLE 8: Scale Factors of the Diagonal Force Constants (FC) of DMP and NaDMP[a]

	DMP			NaDMP	
FC type	HF/3-21G(*)	HF/6-31G*	MP2/6-31+G*	HF/6-31G*	B3-LYP/6-31G*
P−O* stretching	0.74	0.79	0.98	0.87	1.04
P−O stretching	0.90	1.04	1.35	0.87	1.04
C−O stretching	0.81	0.70	0.88	0.73	0.92
OPO bending	0.82	0.85	1.06	0.83 (0.64)[b]	1.05 (0.81)[b]
POC bending	0.82	0.85	1.06	0.93	1.05
CH stretching	0.805	0.80	0.865	0.78	0.88
OCH bending	0.84	0.80	0.94	0.79	0.96
CH_3 bending	0.84 (0.75)[c]	0.80	0.94 (0.88)[c]	0.79	0.90
PO torsion	1.94	1.37	1.06	1.37	1.00
CH_3 torsion	1.2	1.06	1.06	1.06	1.00
PNa stretch				0.70	0.60
O*PNa bending				0.50	0.80
no. of independent scale factors	9	7	8	11	10

[a] The scale factors for interaction FCs are calculated as the geometric mean of the corresponding diagonal scale factors, $S_{ij} = (S_{ii}S_{jj})^{1/2}$. [b] The δ(PO12) force constant is scaled separately by the scale factor given in parentheses. [c] The δ(CHa) (asym bending of CH_3 group) force constants are scaled separately by the scale factor given in parentheses.

torsions around PO3 and PO4 bonds. Two differences between the MP2 and B3-LYP results can be found in the 300−600 cm^{-1} region. They concern the interpretation of the 240 cm^{-1} band, observed in solid NaDMP, and the interchanged assignment of the adjacent 367 and 393 cm^{-1} spectral bands (Raman, NaDMP solution). In these cases, the observed intensities and ^{13}C frequency shifts support the DMP-based MP2 assignments. On the other hand, the observation of the band near 270 cm^{-1} can only be explained using the NaDMP model. It should also be noted that the MP2 assignments completely agree with the results of empirical normal coordinate analysis carried out recently by Thomas et al.[8]

The bands in the *700−900 cm^{-1} frequency region* belong to the in-phase (symmetric) and out-of-phase (antisymmetric) stretching vibrations of the PO3 and PO4 bonds. Our assignment is clearly supported by the agreement in observed and calculated intensities and depolarization ratios. The symmetric PO stretching band (ν_s(PO)) dominates the Raman spectrum of NaDMP. Its frequency is calculated to increase by 13 cm^{-1} upon gg → gt conformational transition (Table 10). Indeed, the frequency of this band was observed to be significantly sequence-dependent in Raman studies of synthetic oligonucleotides.[1,2] However, the present model is still too simple to be able to quantitatively explain these experimental findings. To improve the model, the coupling with vibrations of sugars, and the strain exerted on phosphate by structural requirements for optimal interbase and inter-phosphate interactions, should be taken into account.

The strong IR doublet and two weak Raman bands are observed and calculated to lie near *1050 cm^{-1}*. These bands are unambiguously assigned to the in-phase and out-of-phase combinations of stretching vibrations of O3−C3 and O4−C4 bonds. Relative IR intensities of these two bands are significantly improved in NaDMP model compared to DMP. The remaining discrepancy between the nearly equal observed IR intensity of these bands and the predicted 4-fold intensity difference is probably caused by environmental effects that were not accounted for in our calculations. The IR intensity difference between these bands further increase upon going from gg to gt and tt conformers of NaDMP (Table 10), excluding thus the possible presence of the gt conformation in solid NaDMP.

Stretching vibrations of the P−O1 and P−O2 bonds, along with CCH rocking, determine the spectral pattern observed in the *1070−1300 cm^{-1} region*.. The lower frequency component, i.e., the in-phase PO* stretching vibration (ν_s(PO*)), is observed to have high IR and Raman intensity. The out-of-phase PO* stretching band (ν_a(PO*)) is strong in the IR spectra but weak in the Raman spectra of NaDMP. This intensity behavior is well reproduced by our calculations. However, the frequencies of these two bands, and mainly the gap between them, cannot be predicted accurately enough within the SQM methodology. The reason for such difficulties stems from the lack of explicit solvation effects in our computational model. Indeed, the observed frequencies of ν_s(PO*) and ν_a(PO*) bands are strongly environmentally sensitive, as revealed by Raman spectra of aqueous solution and solid NaDMP (Figures 3 and 4). The measured frequency difference between the ν_s(PO*) and ν_a(PO*) bands in solid and aqueous solution amounts to 121−128 cm^{-1}. The SQM calculation based on DMP and NaDMP force fields provide too large (198 cm^{-1}) or too small (108 cm^{-1}) frequency gap, respectively (Table 9). We would like to point out here that the calculated frequency gaps are virtually independent of scaling, since the same scale factors are used for the internal coordinates of the same type. Interestingly enough, the reverted dependence upon the presence of Na^+ is found for ν_s(PO) and ν_a(PO) bands. Experimentally, a 49−72 cm^{-1} frequency gap is observed between these two modes, whereas MP2 (DMP) and B3-LYP (NaDMP) results underestimate (33 cm^{-1}) and overestimate (82 cm^{-1}) this difference, respectively. Obviously, the explicit inclusion of Na^+ in calculations improves the calculated frequency gaps. However, the residual discrepancies between experimental data and NaDMP-based calculations indicate that phosphate−counterion interactions are overestimated in NaDMP, probably due to the disregarded interactions with solvent molecules.

Bending vibrations of methyl groups, located in the *1400−1500 cm^{-1} frequency region*, were not of immediate interest in this study, because they are replaced by ribose atoms in nucleic acids. Nevertheless, it is worth noting that computational methods used by us failed in predicting Raman intensities of these modes. In particular, while only a broad weak doublet was observed in this region, two bands with Raman intensity comparable with the strong ν_s(PO*) band were calculated. This discrepancy can be attributed in part to the C_2 symmetry of isolated NaDMP. In solid or liquid state, where the ideal C_2 symmetry is lost, intensity is redistributed among all CH_3 bending modes lying in this region. As a result, a broad band is observed. Another source of this discrepancy is probably due to the insufficient basis set size. Indeed, in our calibration study of Raman spectra of ethane, we found intensities of the CH_3 bending vibrations to be very sensitive to the basis set extension.[59] In this study, the complete agreement with experiment data on gaseous ethane was obtained only when the

TABLE 9: Experimental and Calculated[a] Vibrational Spectra of Sodium Dimethyl Phosphate in Solid State and Aqueous Solution

frequency (intensity)[b]						$\Delta\nu^{13}$C (cm^{-1})[c]			depolarization ratio			assignment(PED (%)[d])	
IR solid	IR solution	Raman solid	Raman solution	mp2	b3lyp	exp	mp2	b3lyp	exp	mp2	b3lyp	mp2	b3lyp
					77 (25, 1.5)			1		0.00	0.75		δ(PNa2)(69) − τ_a(PO)(18)
		75 w[e]		88 (4.5, 21)	86 (2.1, 14)		2	2		0.75	0.75	τ_s(PO)(84)	τ_s(PO)(88)
		108 m[e]		114 (0.6, 1.8)	103 (4.2, 0.4)		0	0		0.75	0.75	τ_a(PO)(50) + τ_a(CH)(46)	τ_a(PO)(56) + δ(PNa2)(23)
148 w[e]				134 (0.4, 11)	136 (0.0, 5.8)		0	1		0.74	0.74	τ_sCH(84)	τ_sCH(90)
		167 w		167 (2.1, 6.1)	150 (7.3, 5.4)		1	1		0.75	0.75	τ_a(CH)(48) − τ_a(PO)(46)	τ_a(CH)(62)
197 w		208 w			185 (9.7, 0.7)			2			0.75		δ(PNa1)(36) + δ(POr)(19)
217 w		233 w		233 (4.9, 12)	216 (2.9, 13)		2	3		0.38	0.27	δ_s(OC)(46) − δ(POt)(42)	δ_s(OC)(52) − δ(POt)(35)
		248 w		248 (6.5, 9.4)	246 (44, 15)		4	0		0.75	0.11	δ_a(OC)(64) + δ(POr)(33)	ν(PNa)(84)
264 w		262 w			273 (11, 2.8)			2			0.75		δ_a(OC)(50) − δ(PNa1)(43)
377 m		367 m	370 w	363 (0.3, 17)	363 (6.4, 22)	0	0	3	0.63	0.74	0.38	δ(PO34)(49) + δ(PO12)(34)	δPOt(54) + δPO34(21)
409 m		403 m	394 w	387 (18, 29)	397 (30, 9.0)	4	4	1	0.53	0.29	0.73	δ(POt)(46) + δ_s(OC)(32)	δ(PO34)(29) + δ(PO12)(44)
491 m		489 m	478 w	456 (35, 34)	454 (39, 31)	5	3	3	0.55	0.75	0.75	δPOw(70)	δPOw(71)
524 w		528 m	517 sh	528 (46, 21)	522 (51, 17)	2	0	1	0.48[f]	0.72	0.74	δ(PO12)(44) − δ(PO34)(27)	δ(PO12)(49) − δ(PO34)(25)
566 m		564 m	543 w	545 (34, 19)	545 (22, 16)	2	1	0	0.69	0.75	0.75	δ(POr)(45) − δ(POw)(24)	δ(POr)(48) − δ(POw)(21)
755 m		755 s	753 s	766 (40, 165)	741 (23, 169)	4	4	4	0.03	0.02	0.01	ν_s(PO)(62) + ν_s(OC)(20)	ν_s(PO)(60) + ν_s(OC)(18)
807 s		804 w	825 w	799 (244, 33)	823 (209, 32)	5	2	2	0.67	0.75	0.75	ν_a(PO)(70) + δ(POw)(14)	ν_a(PO)(64) + δ(POw)(19)
1042 s	1038 s	1038 w	1034 sh	1044 (236, 31)	1044 (299, 21)	13	15	15	0.7[f]	0.75	0.75	ν_a(OC)(78) − ν_a(PO)(12)	ν_a(OC)(74) − ν_a(PO)(16)
1065 s	1060 sh	1071 w	1059 sh	1058 (23, 13)	1056 (82, 20)	9	14	16	0.2[f]	0.66	0.40	ν_s(OC)(70) − ν_s(PO*)(18)	ν_s(OC)(76)
1116 s	1084 s	1127 s	1083 s	1078 (372, 92)	1105 (416, 67)	2	1	1	0.08	0.12	0.08	ν_s(PO*)(62) − ν_s(PO)(16)	ν_s(PO*)(74) − ν_s(PO)(10)
				1162 (0.8, 11)	1164 (1.8, 7.4)		8	8		0.75	0.75	δ_a(CHr1)(72)	δ_a(CHr1)(74)
		1163 w	1159 w	1162 (0.4, 24)	1164 (0.2, 20)	8	8	8	0.78	0.73	0.71	δ_s(CHr1)(80)	δ_s(CHr1)(82)
1189 m	1188 sh	1192 m	1186 w	1186 (23, 6.8)	1186 (28, 5.0)	12	9	8	0.78	0.75	0.75	δ_a(CHr2)(66)	δ_a(CHr2)(66)
				1189 (33, 16)	1187 (22, 13)		9	8		0.55	0.47	δ_s(CHr2)(68)	δ_s(CHr2)(76)
1244 s	1208 s	1248 w	1206 w	1276 (331, 20)	1213 (270, 18)	4	0	0	0.64	0.75	0.75	ν_a(PO*)(92)	ν_a(PO*)(90)
1450 w	1450 w	1450 w	1448 m	1441 (3.0, 1.1)	1419 (0.0, 15)		2	5		0.75	0.50	δ_a(CHa1)(58) − δ_a(CHa2)(28)	δ_s(CHs)(94)
				1442 (0.2, 90)	1423 (1.5, 5.6)		2	5		0.74	0.75	δ_s(CHa1)(58) − δ_s(CHa2)(30)	δ_a(CHs)(92)
				1453 (1.4, 25)	1447 (0.8, 91)	6	5	2	0.57	0.66	0.74	δ_s(CHs)(70)	δ_s(CHa1)(68)
				1459 (6.0, 5.9)	1448 (3.8, 4.1)		5	2		0.75	0.75	δ_a(CHs)(60) + δ_a(CHa1)(24)	δ_a(CHa1)(64)
1466 w	1465 w	1467 w	1463 m	1470 (5.5, 3.0)	1460 (8.1, 2.3)		3	3		0.75	0.75	δ_a(CHa2)(50) − δ_a(CHs)(32)	δ_a(CHa2)(64)
				1475 (2.7, 54)	1464 (4.7, 64)	2	3	6	0.78	0.74	0.73	δ_s(CHa2)(54) − δ_s(CHs)(24)	δ_s(CHa2)(66)
				2850 (84, 0.0)	2860 (50, 3.0)		3	3		0.75	0.75	ν_a(CHs)(96)	ν_a(CHs)(94)
2849 w	2855 w	2849 s	2854 s	2850 (99, 469)	2861 (48, 399)	5	2	3	0.05	0.01	0.01	ν_s(CHs)(96)	ν_s(CHs)(94)
2915 w	2913 w	2916 sh	2912 sh	2925 (110, 175)	2927 (47, 91)	8	11	11	0.23[f]	0.75	0.75	ν_a(CHa2)(78)	ν_a(CHa1)(56) + ν_a(CHa2)(40)
2951 w	2957 w	2952 s	2957 s	2926 (0.4, 51)	2928 (15, 58)	6	11	11	0.06	0.20	0.49	ν_s(CHa2)(80)	ν_s(CHa1)(56) + ν_s(CHa2)(40)
2982 w		2999 sh	2995 sh	2946 (28, 121)	2954 (38, 139)	10	11	11	0.7[f]	0.75	0.75	ν_a(CHa1)(80)	ν_a(CHa2)(54) − ν_a(CHa1)(44)
3003 w			3020 w	2946 (41, 110)	2954 (19, 106)	11	10	11	0.6[f]	0.72	0.47	ν_s(CHa1)(80)	ν_s(CHa2)(54) − ν_s(CHa1)(42)

[a] SQM MP2/6-31+G* force field of gg conformer of DMP (mp2) and SQM B3-LYP/6-31G* force field of gg conformer of NaDMP (b3lyp). For scale factors see Table 8. [b] Frequency (cm^{-1}) (IR intensity (km/mol), Raman differential crossection (10^{-36} m^2 sr^{-1})). Experimental intensities are abreviated as s (strong), m (meidum), w (weak), sh (shoulder). mp2 and b3lyp Raman intensities were calculated from mp2 and b3lyp normal modes combined with HF/6-31++G**//MP2/6-31+G* and HF/6-31++G**//B3-LYP/6-31G* Cartesian polarizability derivatives, respectively. [c] Experimental ^{13}C frequency shifts were determined as average of the shifts in the Raman spectra of solution and crystalline samples (ref 8). [d] Potential energy distribution (PED) is given in terms of internal coordinates observing C_2 symmetry. These coordinates were formed as symmetric (s) and antisymmetric (a) combinations of the internal coordinates given in Table 5. For example, τ_s(PO) = τ(PO3) + τ(PO4), τ_a(PO) = τ(PO3) − τ(PO4). [e] Barium dimethyl phosphate (ref 7). These data were not used for calculation of scale factors. [f] Reference 8.

TABLE 10: Prediction of the Conformation-Dependent Changes of the Diagnostic IR and Raman Bands of NaDMP[a]

frequency (cm^{-1})					IR intensity (km/mol)			Raman intensity[b]			
exp[c]	gg-DMP[d]	gg	gt	tt	gg	gt	tt	gg	gt	tt	assignment
754	766	750	764	784	19	53	79	171	163	188	ν_s(PO)
816	794	824	831	827	247	188	96	34	29	1.5	ν_a(PO)
1038	1047	1041	1048	1048	395	505	835	19	27	22	ν_a(OC)
1062	1065	1057	1071	1089	124	105	42	24	22	48	ν_s(OC)
1100	1080	1115	1110	1106	443	391	241	80	71	66	ν_s(PO*)
1225	1277	1221	1202	1179	417	429	400	18	20	11	ν_a(PO*)

[a] HF/6-31G* force field scaled by scale factors given in Table 8. IR and Raman intensities were calculated from the SQM HF/6-31G* force field and HF/6-31+G** atomic polar tensors and polarizability derivatives, respectively. Both the force fields and intensity parameters were evaluated in HF/6-31G* optimized geometry. [b] Raman differential crossection (10^{-36} m^2/sr) calculated for excitation wavelength of 488 nm and temperature 300 K. [c] Mean value of band frequency from IR spectrum of solid NaDMP and Raman spectrum of aqueous solution of NaDMP (Table 9). [d] SQM HF/6-31G* frequencies of DMP in gg conformation.

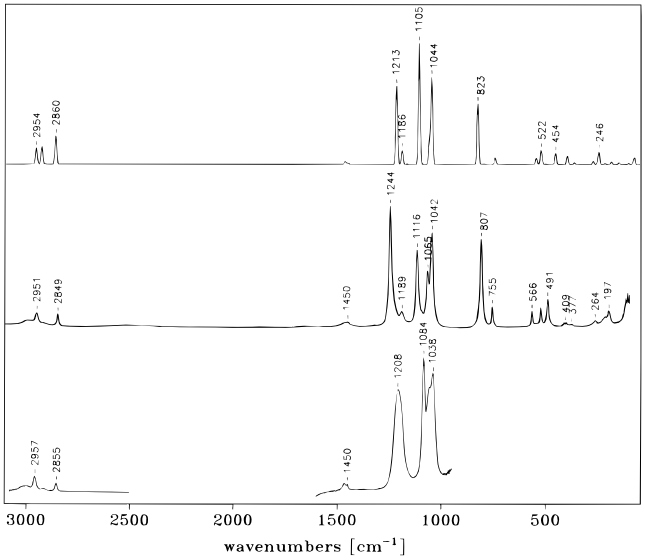

Figure 3. Infrared spectra of sodium dimethyl phosphate. (Top) Spectrum calculated by using SQM B3-LYP/6-31G* force field of *gauche*−*gauche* conformer of NaDMP. (Middle) FTIR spectrum in KBr (4000−400 cm^{-}) and CsI (400−100 cm^{-1}) pellets. (Bottom) FTIR spectrum of 1 M solution in H_2O measured in a 6 μm cell with CaF_2 windows.

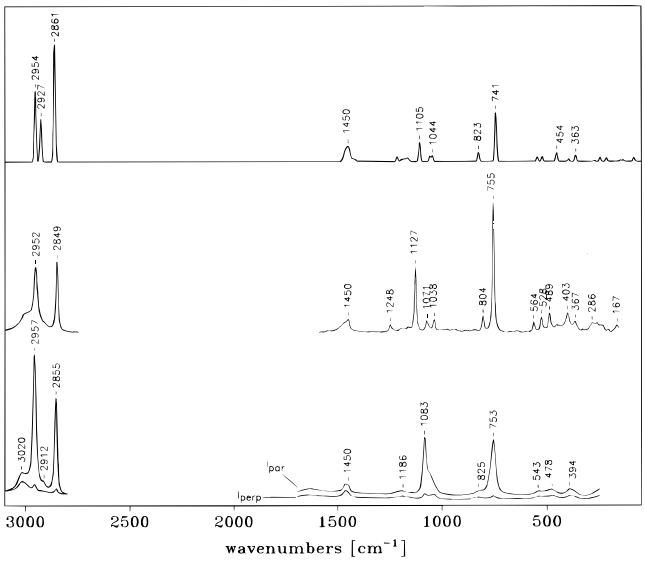

Figure 4. Raman spectra of sodium dimethyl phosphate. (Top) Spectrum calculated using an SQM B3-LYP/6-31G* force field of *gauche*−*gauche* conformer of NaDMP. (Middle) Raman spectrum of polycrystalline solid. (Bottom) Polarized Raman spectra ($I_{\parallel}$ and $I_{\perp}$) of 1 M solution in H_2O.

basis set of the TZ quality augmented by very diffuse polarization functions was used, while smaller basis set provided overestimated Raman intensities of CH_3 bending vibrations.

In the *CH stretching region (2800−3100 cm^{-1})*, the spectral interpretation based on harmonic approximation is hindered by the appearance of Fermi resonance between CH stretching and bending modes. For a more detailed discussion on this topic we refer the reader to the paper by Thomas et al.[8]

The calculated *conformational sensitivity of the vibrational spectra* of NaDMP is given in Table 10. As we have already mentioned, caution should be taken in attempts to use the calculated spectral variations for interpretation of the conformational and sequence dependence of the vibrational spectra of nucleic acids. However, because of the fairly characteristic nature of the vibrational spectra of DMP and NaDMP, the influence of the Na^+−DMP interactions on the conformation-induced spectral variations can be evaluated. In this respect, the comparison between HF/6-31G* frequency shifts calculated for DMP[13] and NaDMP (Table 10) reveals that similar frequency shifts occur for diagnostic PO*, PO, and CO stretching modes in both systems. This is an important finding underlying the applicability of methods of vibrational spectroscopy to the study of DNA conformations. If conformation-dependent frequency shifts differed for DMP and NaDMP, theory might not be able to provide unique interpretation of measured conformation-dependent spectral variations. This statement is based on the fact that solvation of native DNA phosphate groups is not homogeneous. Different counterions are often involved, and their positions strongly fluctuate with time. Thus, spectra averaged over large number of phosphate groups in different environments are measured. As a result, spectrum−conformation relationships can be studied only when conformation-dependent frequency and intensity changes for differently solvated phosphates exhibit the same trend.

Conclusions

In this study, we expanded the set of available experimental data on NaDMP by measuring IR spectrum of its 1 M aqueous solution. The IR and Raman spectra of solid NaDMP as well as Raman spectrum of aqueous solution of NaDMP measured by us closely resemble the spectra reported previously by Thomas et al.[8] The calculated spectra are in good agreement with observed data, including the IR and Raman intensities. Thus, the suggested band assignments can be considered to be highly plausible.

Three nonequivalent minima on the potential energy surface of DMP and NaDMP, and three transition states on the reaction path connecting them, were located by Hartre−Fock and gradient-corrected density functional calculations. In addition, results of our quantum chemical calculations indicated that interactions of phosphate anion with Na^+ have only small effects upon the flexibility of dimethyl phosphate. Also, electron

correlation was shown to influence only marginally torsional angles and relative energies of different minima and transition states of DMP and NaDMP. Finally, the conformational transitions have been shown to influence the force fields and vibrational spectra of the anionic and neutralized phosphate group in a similar manner. These findings provide a certain credit to the models of DNA phosphate groups that disregard counterion atoms. In addition, because different phosphate groups in native DNAs form often complexes with cations of different types, or they remain negatively charged, cation independence of the spectra−conformation relationship, demonstrated by us, is a necessary condition for the use of bands of phosphodiester moiety as marker bands in studies of DNA polymorphism by vibrational spectroscopy.

The complex with sodium cation must be treated explicitly when the frequencies of symmetric and antisymmetric stretching vibrations of anionic oxygens (O*−P−O*) need to be predicted with a higher degree of sophistication. Also, the proper description of long-range electrostatic interactions may require the use of atomic charges developed for the sodium dimethyl phosphate.

The scaled (SQM) harmonic force fields based on Hartree−Fock approximation can provide reliable vibrational spectra of title compounds. However, we recommend the scaled force fields based on the B3-LYP/6-31G* density functional calculations as a method of choice for predicting vibrational spectra of DNA fragments containing phosphate groups. Given the use of the B3-LYP method is more economical for large systems than conventional post-Hartree−Fock calculations, highly reliable SQM B3-LYP interpretations of vibrational spectra of nucleotides may be feasible in the near future.

Acknowledgment. This work was supported by the Grant Agency of the Czech Republic (No. 203/93/2362). The calculations were carried out at the Supercomputing Center of Charles University, Prague, Army High Performance Computing Research Center (founded by the contract DAAH 04-95-C-0008 between the Army Research Office and the University of Minnesota), and the Theoretical Department of the Institute of Physics, Prague. The kind help of Prof. Ivan Barvík, Prof. Jerzy Leszczyński, Dr. Richard P. Muller, Dr. Ivan Rosenberg, and Dr. Zdeněk Točík is gratefully acknowledged.

References and Notes

(1) Thomas, Jr., G. J.; Tsuboi, M. *Adv. Biophys. Chem*. **1993**, *3*, 1.
(2) Peticolas, W. L.; Evertsz, E. *Methods Enzymol*. **1992**, *211*, 335.
(3) Taillandier, E.; Liquier, J. *Methods Enzymol*. **1992**, *211*, 307.
(4) Shimanouchi, T.; Tsuboi, M.; Kyogoku, Y. *Adv. Chem. Phys.* **1964**, *7*, 435.
(5) Brown, E. B.; Peticolas, W. L. *Biopolymers* **1975**, *14*, 1259.
(6) Bicknell-Brown, E.; Brown, K. G.; Person, W. B. *J. Raman. Spectrosc*. **1982**, *12*, 180.
(7) Taga, K.; Miyagai, K.; Hirabayashi, N.; Yoshida, T.; Okabayashi, H. *J. Mol. Struct*. **1991**, *245*, 1.
(8) Guan, Y.; Wurrey, C. J.; Thomas, Jr., G. J. *Biophys. J.* **1994**, *66*, 225.
(9) Garrigou-Lagrange, C.; Bouloussa, O.; Clement, C. *Can. J. Spectrosc*. **1976**, *21*, 75.
(10) Okabayashi, H.; Yoshida, T.; Ikeda, T.; Matsuura, H.; Kitagawa, T. *J. Am. Chem. Soc*. **1982**, *104*, 5399.
(11) Lu, K. C.; Prohofsky, E. W.; Zandt, L. L. V. *Biopolymers* **1977**, *16*, 2491.
(12) Hadzi, D.; Hodoscek, M.; Grdadolnik, J.; Avbelj, F. *J. Mol. Struct.* **1992**, *266*, 9.
(13) Liang, C.; Ewig, C. S.; Stouch, T. R.; Hagler, A. T. *J. Am. Chem. Soc*. **1993**, *115*, 1537.
(14) Pulay, P.; Meyer, W. *Mol. Phys.* **1974**, *27*, 473.
(15) Blom, C. E.; Altona, C. *Mol. Phys*. **1976**, *31*, 1377.
(16) Pulay, P.; Fogarasi, G.; Pongor, G.; Boggs, J. E.; Vargha, A. *J. Am. Chem. Soc*. **1983**, *105*, 7073.
(17) Pulay, P.; Fogarasi, G.; Pang, F.; Boggs, J. E. *J. Am. Chem. Soc*. **1979**, *101*, 2550.
(18) Fogarasi, G.; Pulay, P. In *Vibrational Spectra and Structure*; Durig, J. R., Ed.; Elsevier: Amsterdam, 1985; Vol. 14; pp 125.
(19) (a) Florián, J. *J. Mol. Struct. (THEOCHEM)* **1992**, *253*, 83. (b) Florián, J.; Mojzes, P.; Stepánek, J. *J. Phys. Chem*. **1992**, *96*, 9278.
(20) Florián, J.; Hrouda, V. *Spectrochim. Acta* **1993**, *49A*, 921.
(21) Florián, J.; Baumruk, V. *J. Phys. Chem*. **1992**, *97*, 9283.
(22) Florián, J. *J. Phys. Chem*. **1993**, *97*, 10649.
(23) Florián, J.; Baumruk, V.; Leszczynski, J. *J. Phys. Chem.*, submitted.
(24) Guan, Y.; Choy, G. S.-C.; Glaser, R.; Thomas, Jr., G. J. *J. Phys. Chem*. **1995**, *99*, 12054.
(25) Saenger, W. *Principles of Nucleic Acid Structure*; Springer Verlag: New York, 1984.
(26) Landin, J.; Pascher, I.; Cremer, D. *J. Phys. Chem*. **1995**, *99*, 4471.
(27) Alagona, G.; Ghio, C.; Kollman, P. *J. Am. Chem. Soc*. **1983**, *105*, 5226.
(28) Alagona, G.; Ghio, C.; Kollman, P. A. *J. Am. Chem. Soc*. **1985**, *107*, 2229.
(29) Jayaram, B.; Mezei, M.; Beveridge, D. L. *J. Comput. Chem*. **1987**, *8*, 917.
(30) Jayaram, B.; Mezei, M.; Beveridge, D. L. *J. Am. Chem. Soc*. **1988**, *110*, 1691.
(31) Jayaram, B.; Ravishanker, G.; Beveridge, D. L. *J. Phys. Chem*. **1988**, *92*, 1032.
(32) Dickerson, R. E. *Methods Enzymol*. **1992**, *211*, 67.
(33) Neidle, S. *DNA Structure and Recognition*; Oxford University Press: Oxford, U.K., 1994.
(34) Parr, R. G.; Yang, W. *Density functional theory of atoms and molecules*; Oxford: New York, 1989.
(35) *Density Functional Methods in Chemistry*; Labanowski, J. K., Andselm, J. W., Eds.; Springer: New York, 1991.
(36) Johnson, B. G.; Gill, P. M. W.; Pople, J. A. *J. Chem. Phys*. **1993**, *98*, 5612.
(37) Handy, N. C.; Murray, C. W.; Amos, R. D. *J. Phys. Chem*. **1993**, *97*, 4392.
(38) Florián, J.; Johnson, B. G. *J. Phys. Chem*. **1994**, *98*, 3681.
(39) Florián, J.; Johnson, B. G. *J. Phys. Chem*. **1995**, *99*, 5899.
(40) Rauhut, G.; Pulay, P. *J. Phys. Chem*. **1995**, *99*, 3093.
(41) Frisch, M. J.; Trucks, G. W.; Schlegel, H. B.; Gill, P. M. W.; Johnson, B. G.; M. W. Wong; Foresman, J. B.; Robb, M. A.; Head-Gordon, M.; Replogle, E. S.; Gomperts, R.; Andres, J. L.; Raghavachari, K.; Binkley, J. S.; Gonzalez, C.; Martin, R. L.; Fox, D. J.; Defrees, D. J.; Baker, J.; Stewart, J. J. P.; Pople, J. A. *Gaussian 92/DFT, Revision G*; Gaussian, Inc.: Pittsburgh, PA, 1992.
(42) Becke, A. D. *Phys. Rev*. **1988**, *A38*, 3098.
(43) Lee, C.; Yang, W.; Parr, R. G. *Phys. Rev. B* **1988**, *37*, 785.
(44) Becke, A. D. *J. Chem. Phys*. **1993**, *98*, 5648.
(45) Besler, B. H.; Merz, Jr., K. M.; Kollman, P. A. *J. Comput. Chem*. **1990**, *11*, 431.
(46) Singh, U. C.; Kollman, P. A. *J. Comput. Chem*. **1984**, *5*, 129.
(47) Sundius, T. *J. Mol. Struct*. **1990**, *218*, 321.
(48) Florián, J. *SQMVIB: A computer program for calculation of scaled quantum mechanical vibrational spectra of molecules*; Charles University: Prague, 1994.
(49) Person, W. B. In *Vibrational intensities in infrared and Raman spectroscopy*; Person, W. B., Zerbi, G., Eds.; Elsevier: Amsterdam, 1982.
(50) Amos, R. D. *Chem. Phys. Lett*. **1986**, *124*, 376.
(51) Polavarapu, P. L. *J. Phys. Chem*. **1990**, *94*, 8106.
(52) Kim, S. H.; Berman, M. H.; Seeman, N. C.; Newton, M. D. *Acta Crystallogr*. **1973**, *B29*, 703.
(53) Dickerson, R. E.; Drew, H. R. *J. Mol. Biol*. **1981**, *149*, 761.
(54) Gessner, R. V.; Frederick, C. A.; Quigley, G. J.; Rich, A.; Wang, A. H. J. *J. Biol. Chem*. **1989**, *264*, 7921.
(55) (a) Giarda, L.; Garbassi, F.; Calcaterra, M. *Acta Crystallogr*. **1973**, *B29*, 1826. (b) Kyogoku, Y.; Iitaka, Y. *Acta Crystallogr*. **1966**, *21*, 49.
(56) Stangret, J.; Savoie, R. *Can. J. Chem*. **1992**, *70*, 2875.
(57) Cornell, W. D.; Cieplak, P.; Bayly, C. I.; Gould, I. R.; Merz, Jr., K. M.; Ferguson, D. M.; Spellmeyer, D. C.; Fox, T.; Caldwell, J. W.; Kollman, P. A. *J. Am. Chem. Soc*. **1995**, *117*, 5179.
(58) Pearlman, D. A.; Kim, S. H. *J. Mol. Biol*. **1990**, *211*, 171.
(59) Johnson, B. G.; Florián, J. *Chem. Phys. Lett*., in press.

JP9520299